Applied Catalysis B: Environmental 99 (2010) 170–180

Contents lists available at ScienceDirect

Applied Catalysis B: Environmental

journal homepage: www.elsevier.com/locate/apcatb

Influence of activated carbon in TiO_2 and ZnO mediated photo-assisted degradation of 2-propanol in gas–solid regime

Juan Matos[a], Elisa García-López[b], Leonardo Palmisano[b], Andreína García[a], Giuseppe Marcì[b,*]

[a] Engineering of Materials and Nanotechnology Centre, Venezuelan Institute for Scientific Research, 20632, Caracas 1020-A, Venezuela
[b] Schiavello-Grillone Photocatalysis Group, Dipartimento di Ingegneria Chimica, Viale delle Scienze, Palermo, Italy

ARTICLE INFO

Article history:
Received 23 March 2010
Received in revised form 28 May 2010
Accepted 7 June 2010
Available online 11 June 2010

Keywords:
Activated carbon
Titanium dioxide
Photocatalysis
2-Propanol

ABSTRACT

2-Propanol was photocatalytically oxidized in the presence of binary materials composed by mixtures of home-prepared active carbon and commercial TiO_2 or ZnO. Remarkable beneficial improvements of the photocatalytic activity were observed in the presence of activated carbon (AC). In particular the presence of AC along with TiO_2 in the binary materials enormously increased the photocatalytic ability of the bare semiconductor to completely oxidize the substrate, indicating a synergy between the semiconductor and AC. Probably, when AC was present in the binary materials, the majority of the substrate and of the intermediates were reversibly adsorbed onto the AC surface. Due to the presence of a contact interface between TiO_2 and AC, a continuous transfer of the species from the AC to the TiO_2 surface was possible. On the other hand, the presence of AC avoided the deactivation of TiO_2 that occurred instead for the bare semiconductor. The reaction rate in the presence of ZnO based materials was always lower with respect to that observed for the corresponding TiO_2 ones, although the presence of AC improved the photoactivity of bare semiconductor in this case also.

1. Introduction

Heterogeneous photocatalysis by using polycrystalline semiconductor oxides is a technology that has been applied to degrade organic and inorganic pollutants both in vapour and liquid phases [1–3]. It offers various advantages compared with traditional treatment methods because the photoreactions occur with measurable rates under near-UV radiation at room temperature and atmospheric pressure, giving rise to degradation down to very low concentration levels of refractory, very toxic and non-biodegradable molecules. Many semiconductor materials have been tested as photocatalysts but it is generally accepted that TiO_2, due to its low cost and high activity and stability under irradiation, is the most reliable material [1–3]. A methodology to increase the photocatalytic activity of the semiconductor consists in adding a co-adsorbent, as activated carbon (AC). Bare AC has been proposed as catalyst support [4] due to its high adsorption ability related to its high specific surface area. Binary materials constituted by TiO_2 and AC have already been proposed as photocatalysts in liquid–solid regime to photooxidize organic pollutants as phenol [5], chlorophenol [6,7] and herbicides [8]. A remarkable increase in the activity of TiO_2 has been attributed not only to the high surface area of the composite photocatalyst but also to the low-strength of adsorption that allows the diffusion of the pollutants from the adsorbent, AC, to the TiO_2 phase [8]. Literature suggests that there are no significant changes in the band-gap energy of TiO_2 as a consequence of the interaction AC–TiO_2 [9]. In fact the enhanced photocatalytic activity of the binary AC–TiO_2 materials in liquid–solid systems has been attributed to the interaction between AC and Ti–O bonds [5,10]. On the other hand only few papers reporting the study of ZnO–AC binary materials used as photocatalysts in reactions carried out in liquid phase exist in literature [11]. The main aim of the present study was to investigate the synergy between TiO_2 and AC in a gas–solid system and to relate the physico-chemical features of the solid photomediators with their photocatalytic activity for the degradation of 2-propanol. Moreover, the extension of the study to the binary material ZnO–AC allowed to compare the role played by the semiconductor coupled with AC.

On the other hand 2-propanol is an interesting molecule for photo-oxidation studies, since it may undergo different degradation pathways. The photocatalytic degradation of 2-propanol in the gas–solid regime in the presence of both oxygen and UV light at ambient temperature has been used as a probe reaction in the presence of TiO_2. Propanone is reported by many authors to be the only intermediate in the photocatalytic oxidation of 2-propanol both in gas–solid [12–15] and in liquid–solid regimes [16–18], followed by subsequent photo-oxidation to produce ultimately CO_2. Nevertheless the use of modified TiO_2, for instance by incorporating sulphuric acid during the photocatalyst preparation, leads

* Corresponding author. Tel.: +39 091 23863737; fax: +39 091 7025020.
E-mail address: marci@dicpm.unipa.it (G. Marcì).

0926-3373/$ – see front matter © 2010 Elsevier B.V. All rights reserved.
doi:10.1016/j.apcatb.2010.06.014

to a high selectivity versus the formation of isopropylether [19]. Propene, moreover, was also obtained photocatalytically by using polyoxometalate supported TiO_2 samples, due to their acid surface character [20].

2. Experimental

2.1. Photocatalysts preparation and characterization

Active carbon (AC) was prepared from sawdust of *Tabebuia Pentaphyla* wood by 1 h gasification with CO_2 at 800 and 900 °C. These types of carbon are classified in literature as H-type or close AC [21,22].

The active carbon samples were denoted as AC_{800} and AC_{900}, where the number indicates the activation temperature.

Commercial TiO_2 Degussa P25 and ZnO, provided by the *Standard American Chemical Association*, were impregnated with the home-prepared active carbon by mixing both powders (AC and the semiconductor) in aqueous suspension followed by filtration [21]. The binary powders containing the semiconductor (TiO_2 or ZnO) and the AC were denoted as TiO_2–$AC_{T\text{-}5}$, TiO_2–$AC_{T\text{-}10}$ or ZnO–$AC_{T\text{-}5}$, ZnO–$AC_{T\text{-}10}$ where T corresponds to 800 or 900 °C (the temperature of AC preparation) and the number 5 or 10 indicates the relative amount semiconductor:AC, expressed in mass, i.e. 5:1 or 10:1, respectively.

Textural characterization was performed by N_2 adsorption–desorption at 77 K. The full isotherms in the range of 0.03–630 Torr were measured in a Micromeritics ASAP-2020 instrument. Scanning electron microscopy (SEM) was performed using a FEI quanta 200 ESEM microscope, operating at 20 kV on specimens after coating with a layer of gold. Samples were also characterized by X-ray diffractometry (XRD) recorded at room temperature in the 2θ range from 5° to 90° with the Difrac-Plus program on a D-5005 diffractometer from Siemens using the Cu Kα (1.54056) radiation. XRD patterns were finally processed by means of Eva program. Surface pH (PZC) of bare AC, TiO_2, ZnO and mixture of solids were obtained by the drift method [23] by comparing the pH measured after 48 h stirring (to achieve the equilibrium of charges) with that of initial buffer solutions. Diffuse reflectance spectra of samples (UV–vis/DRS) were recorded in air at ca. 300 K in the wavelength range 250–800 nm, using a Shimadzu UV-2401 PC spectrophotometer with $BaSO_4$ as the reference material.

2.2. Adsorption and photocatalytic activity experiments

A batch cylindrical fixed bed Pyrex photoreactor (V = 150 ml, $\Phi \approx 93$ mm, $h \approx 22$ mm), operating in gas–solid regime, was used. The set-up of the photoreactivity system is reported in Scheme 1.

The photocatalysts have been simply placed inside the photoreactor in the powdered form. The masses of the powders used in the runs were 0.100 and 0.020 g for the bare semiconductors and AC samples, respectively. The masses of the binary powders, instead, were 0.110 or 0.120 g, depending upon the relative ratio semiconductor:AC in the sample, i.e. 10:1 and 5:1, respectively. Different amounts of solid were used during the photocatalytic runs in order to maintain the same amount of semiconductor (0.100 g of TiO_2 or ZnO). In the tightly closed system, and after purging with pure O_2 for 30 min, 10 μl of liquid 2-propanol was injected and vapourized; therefore the initial concentration of 2-propanol was 8.7×10^{-4} M. Some selected runs were carried out in the presence of water vapour (ca. 8.7×10^{-4} M). The reactor, provided with a water refrigerating jacket that allowed to maintain the temperature inside the reactor at ca. 300 K, was illuminated from the top by a SOLARBOX apparatus (CO.FO.ME.GRA.) equipped with a solar simulating lamp (1500 W high pressure Xe lamp). The irradiation

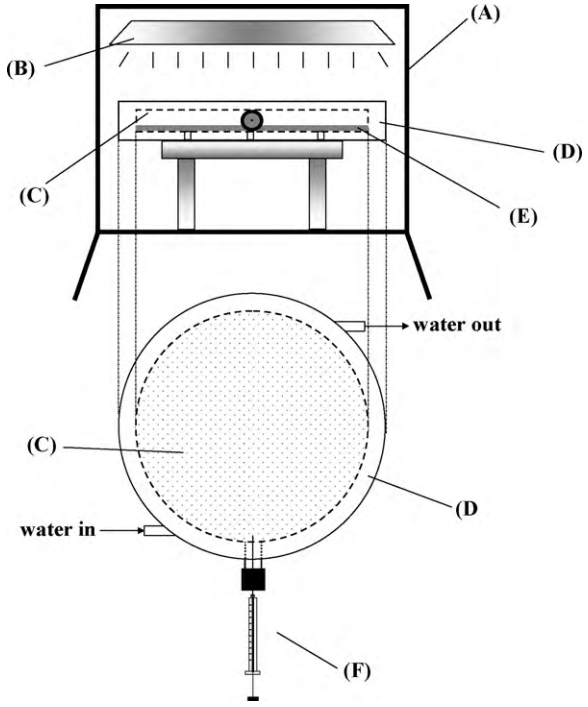

Scheme 1. Set-up of the photoreactive system: (A) SOLARBOX; (B) lamp; (C) photoreactor; (D) water cooling jacket; (E) photocatalyst; and (F) gas-tight syringe.

started only at steady state conditions, after achievement of the adsorption equilibrium of 2-propanol onto the catalysts surface. The irradiance reaching the photoreactor was measured by using a UVX Digital radiometer and it was equal to 1.0 mW cm^{-2}. Samples of the reacting fluid were analyzed by withdrawing 200 μl of gas from the photoreactor by means of a gas-tight syringe. 2-Propanol and intermediates' concentrations were measured by a GC-17A Shimadzu gas chromatograph equipped with an Alltech AT-1 column and a FID, whereas carbon dioxide was analyzed by a Supelco Carboxen 1000 column in a HP6890 gas chromatograph equipped with a TCD.

In order to understand the adsorption ability of the solids, preliminary studies were carried out under dark conditions by using the same experimental set-up showed in Scheme 1. Aliquots of 1 μl of liquid 2-propanol were injected in the tightly closed reactor and after 60 min (time sufficient to reach the adsorption equilibrium) the concentration of 2-propanol in gas phase was measured. The difference between the injected and the measured amounts of 2-propanol was considered the amount adsorbed by the solid. By repeating this operation 10 times, the same amount (10 μl) of 2-propanol used in the photocatalytic runs was injected in the reactor. The amounts of solids employed for these experiments were the same as used in the photocatalytic runs, i.e. 0.110 and 0.120 g. 2-Propanol adsorption ability was also studied for the bare solids, and in these cases the amounts of the solids were 0.100 and 0.020 g for bare semiconductors and AC, respectively.

3. Results and discussion

3.1. Characterization

Fig. 1 shows the N_2 adsorption–desorption isotherms of the bare materials (TiO_2, AC_{800} and AC_{900}). For TiO_2 a type 2 adsorption isotherm with a small and vertical hysteresis phenomenon attributed to aggregation of nanoparticles can be noticed. This isotherm corresponds to a non-porous or relatively large porous material in agreement with the low surface area and the negligi-

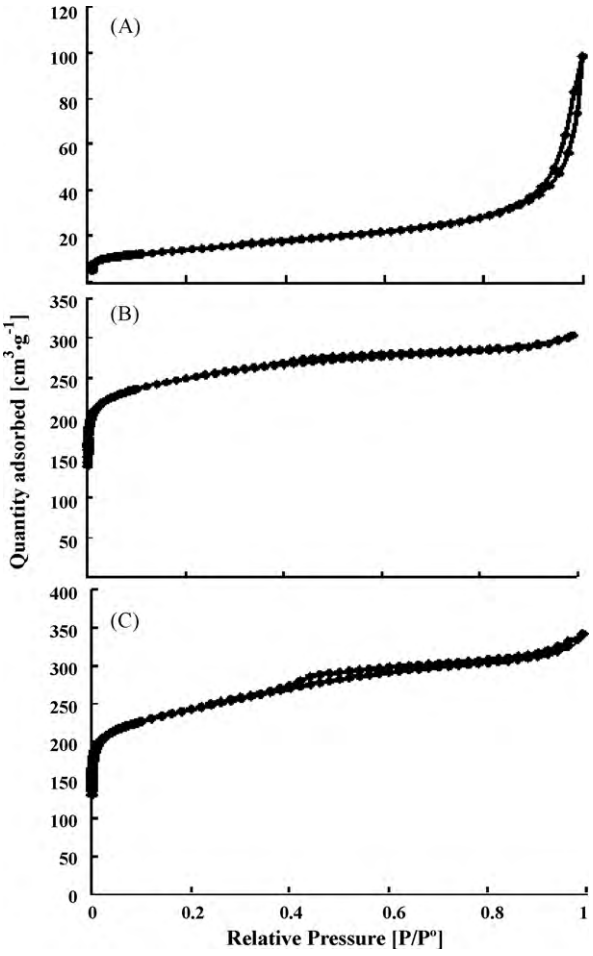

Fig. 1. Adsorption isotherms of bare materials (A) TiO_2 P25; (B) AC_{800}; and (C) AC_{900}.

ble micropore volume and with the large mean pore width values reported in Table 1. Adsorption isotherms of AC_{800} and AC_{900} correspond to a type 1. The framework of these materials is mainly composed of micropores. The small hysteresis in Fig. 1(C) suggests that an important quantity of mesopores is also present in AC_{900}. This is in agreement with the volume of the pores calculated and reported in Table 1 which suggests that the proportion of the micropore volume for AC_{800} is higher with respect to that of AC_{900}. In other words, by comparing V_{micro} with V_{tot}, it can be noticed that AC_{800} is composed by ca. 90% of micropores while AC_{900} only by ca. 80%, in agreement with the higher mean pore width found for AC_{900} (7.7 versus 6.3 Å). This finding can be explained by taking into account the higher activation temperature that induces, probably, the destruction of the micropores. Consequently surface BET area of AC_{900} is lower than that of AC_{800}.

Fig. 2 shows the adsorption–desorption isotherms of the binary materials based on TiO_2. It can be observed that their N_2 adsorption–desorption isotherms are of type 2. This result was expected because the main component of the binary materials is TiO_2.

Moreover this behaviour is in agreement with the moderate S_{BET} values reported in Table 1 for these samples. It is worth noting that both TiO_2–AC_{900} samples present higher S_{BET} values than the TiO_2–AC_{800} ones, but AC_{800} presents a higher specific surface area than AC_{900}. This insight could be associated with the fact that AC_{900} has a higher PZC than AC_{800} (9.1 against 8.5, Table 1) suggesting that the higher the PZC of active carbons the higher the dispersion of TiO_2 nanoparticles in agreement with previous reports [10,21]. As expected, the higher the proportion of carbon, the higher the surface area of the binary materials. In fact, TiO_2–$AC_{800\text{-}5}$ and TiO_2–$AC_{900\text{-}5}$ present higher surface areas than do TiO_2–$AC_{800\text{-}10}$ and TiO_2–$AC_{900\text{-}10}$ samples (see Table 1).

As far as ZnO and ZnO–AC materials are concerned, the trends of the values of the specific surface areas are very similar to those of TiO_2–AC. The N_2 adsorption–desorption isotherms corresponding to ZnO and ZnO–AC materials are not reported because it was impossible to determine the full isotherms due to the micro particle size and the non-porous characteristics of ZnO and ZnO–AC samples.

Therefore, only five points surface BET areas were performed to obtain the basic textural parameters of ZnO and ZnO–AC materials. Some textural properties, i.e. specific surface area (S_{BET}), micropore area (S_{micro}), total pore volume (V_{tot}), micropore volume (V_{micro}) and mean pore width (W_{pore}) are summarized in Table 1.

The results indicate that ZnO is a non-porous material with a very low surface area and a negligible micropore volume. Not only do ZnO–$AC_{800\text{-}5}$ and ZnO–$AC_{900\text{-}5}$ present higher S_{BET} values than ZnO–$AC_{800\text{-}10}$ and ZnO–$AC_{900\text{-}10}$, respectively, but also ZnO–AC_{900} materials show higher S_{BET} values with respect to the ZnO–AC_{800} ones, in agreement with the fact, already discussed in the case of the TiO_2 based samples, that the higher the PZC of AC the higher the surface area of the binary materials.

For the bare AC powders, the higher the activation temperature during the preparation the higher the PZC, indicating the presence of more basic functional groups on the surface of AC, as already reported [21]. The PZC values of TiO_2 and ZnO reported in Table 1 are 6.5 and 9.1, respectively. These values are in accord with those reported for TiO_2 [21] and for ZnO [24]. In consequence, TiO_2–AC binary materials show slightly acidic or close to neutral PZC val-

Table 1
Summary of textural and physico-chemical properties of the materials: BET surface area (S_{BET}), micropore area (S_{micro}), total pore volume (V_{tot}), micropore volume (V_{micro}), and mean pore width (W_{pore}), surface pH (pH_{PZC}) and energy band-gap (E_{bg}).

Samples	S_{BET} ($m^2\ g^{-1}$)	S_{micro}[a] ($m^2\ g^{-1}$)	V_{tot}[b] ($cm^3\ g^{-1}$)	V_{micro}[a] ($cm^3\ g^{-1}$)	W_{pore}[b] (Å)	pH_{PZC}	E_{bg} (eV)
AC_{800}	943	913	0.470	0.409	6.3	9.1	–
AC_{900}	907	858	0.528	0.419	7.7	8.5	–
TiO_2 P25	45.2	nd[c]	0.153	0.002	578	6.5	3.00
TiO_2–$AC_{800\text{-}10}$	86.5	49.2	0.375	0.026	974	6.7	2.93
TiO_2–$AC_{800\text{-}5}$	135	104	0.359	0.048	946	6.9	2.90
TiO_2–$AC_{900\text{-}10}$	91.0	44.5	0.461	0.028	1005	6.8	2.92
TiO_2–$AC_{900\text{-}5}$	145	89.0	0.439	0.045	909	7.1	2.98
ZnO	6.2	nd[c]	nd[c]	nd[c]	nd[c]	9.1	3.23
ZnO–$AC_{800\text{-}10}$	45.9	nd[c]	nd[c]	nd[c]	nd[c]	9.0	3.24
ZnO–$AC_{800\text{-}5}$	86.2	nd[c]	nd[c]	nd[c]	nd[c]	9.0	3.24
ZnO–$AC_{900\text{-}10}$	68.4	nd[c]	nd[c]	nd[c]	nd[c]	9.1	3.24
ZnO–$AC_{900\text{-}5}$	133	nd[c]	nd[c]	nd[c]	nd[c]	9.1	3.24

[a] Obtained from *t*-plot method.
[b] Obtained from Horwath–Kawazoe method.
[c] Not determined.

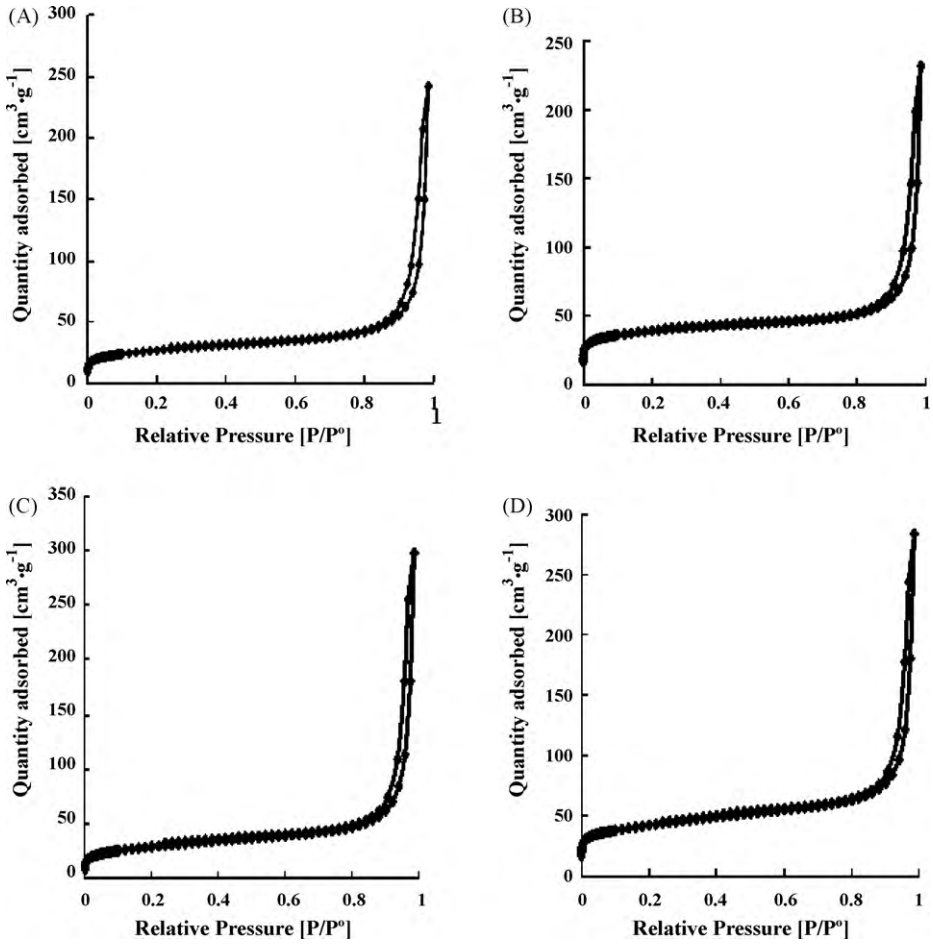

Fig. 2. Adsorption isotherms of (A) TiO_2–$AC_{800\text{-}10}$; (B) TiO_2–$AC_{800\text{-}5}$; (C) TiO_2–$AC_{900\text{-}10}$; and (D) TiO_2–$AC_{900\text{-}5}$.

ues. On the contrary the PZCs of ZnO–AC binary materials are basic. It can be noted, in addition, that the PZCs of TiO_2–AC samples are higher than the value of bare TiO_2 while PZCs of ZnO–AC samples are smaller or virtually identical to that of bare ZnO. The above results suggest a more efficient surface interaction between TiO_2 and AC, probably by means of a common contact interface [5,9,21]. SEM investigation confirms this hypothesis (see Figs. 3 and 4). Indeed TiO_2 P25 appears well deposited onto the activated carbon surface and the amount of TiO_2 present onto carbon is obviously more abundant for the sample in which the nominal ratio TiO_2:AC is higher (10:1). On the contrary, ZnO does not result well deposited onto the AC surface. The majority of ZnO particles results separated from the AC and some aggregates of ZnO are not attached to the AC material.

Fig. 5 shows that the XRD patterns of AC_{800} and AC_{900} present very broad peaks suggesting a very amorphous carbon structure in agreement with the high surface area values for these materials (Table 1). However, a pseudo-graphite crystalline ordering can be suggested, due to the presence of two peaks at diffraction angles 23.0° and 43.7° corresponding to 002 and 101 crystalline faces. On the other hand, XRD patterns of TiO_2 P25 and TiO_2–AC binary materials (not shown for the sake of brevity) indicate the presence of a mixture of anatase and rutile phases, typical of P25 commercial powder [25]. Finally, the XRD pattern of ZnO (not shown for the sake of brevity) indicates the presence of the crystalline zincite structure [24]. The presence of AC did not influence the crystallinity both of TiO_2 and ZnO.

Fig. 6 shows the diffuse reflectance spectra in air of bare TiO_2, TiO_2–AC, bare ZnO and ZnO–AC samples, recorded in the 250–800 nm wavelength range. The spectra always show the typical broad absorption band, ascribed to the charge transfer process from O^{2-} to Ti^{4+} or Zn^{2+} responsible for the band-gap. The band-gap energies of the samples (TiO_2 is an indirect semiconductor and ZnO a direct one [26,27]), estimated from the tangent lines in the plots of the modified Kubelka–Munk function, versus the energy of exciting light [28] were in the 3.0–3.2 eV range. A decrease in reflectance (i.e. increase in absorbance) in the visible region can be observed by adding AC to both the bare semiconductors, i.e. they reflect light less significantly than the bare semiconductors and their absorption increases by increasing the AC amount. The Kubelka–Munk plots showed no significant shift of the binary materials with respect to the bare band-gap edge of TiO_2 or ZnO.

The experimental band-gap of the powders, obtained by the Kubelka–Munk plots, is reported in Table 1. The slight modification can be attributed to the AC H-type solids, that develop a topological structure slightly similar to that of graphite [21] with very well ordered graphene layers. This structural order can influence the electronic density of the AC material increasing their electronic conductivity.

3.2. Adsorption ability of 2-propanol in dark conditions

In order to study the adsorption of 2-propanol onto the surface of the solids, preliminary studies have been carried out in dark conditions. Fig. 7(A)–(C) reports adsorbed 2-propanol onto the solid surface in dark conditions versus 2-propanol injected into the reactor.

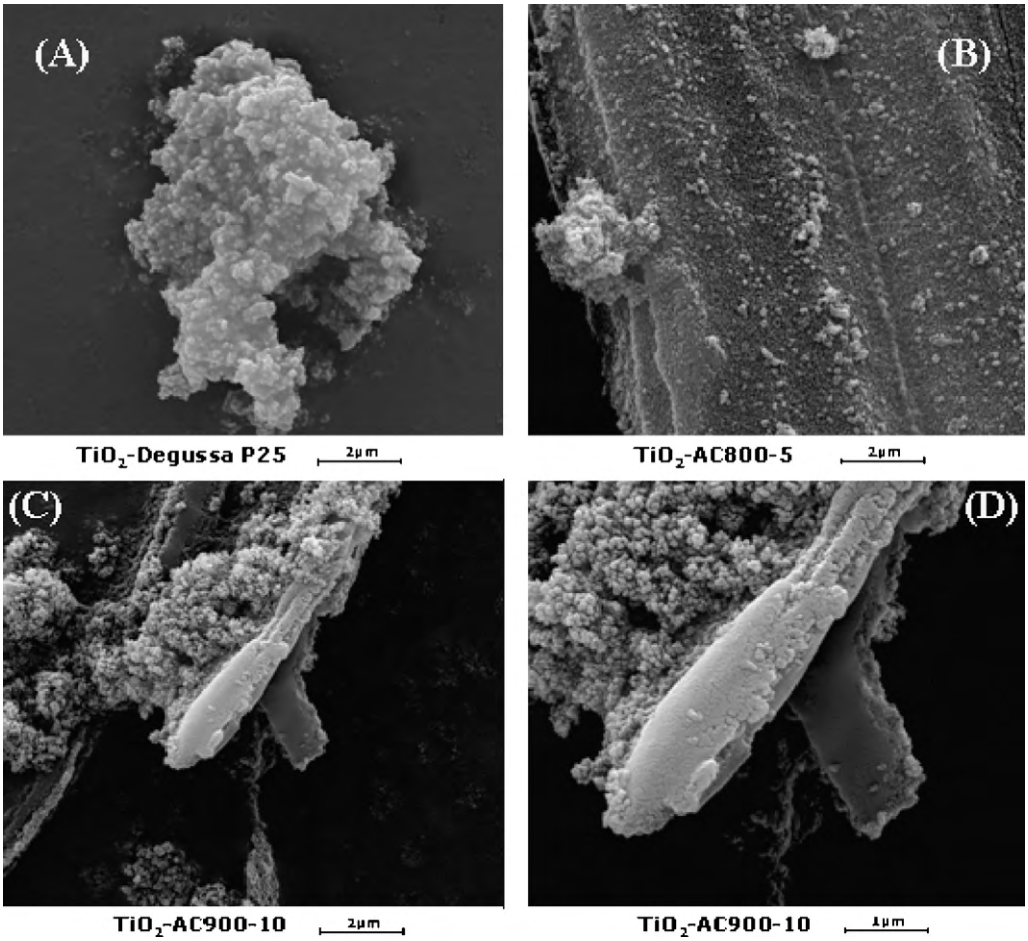

Fig. 3. SEM micrographs of (A) bare TiO_2; (B) TiO_2–$AC_{800\text{-}5}$; (C) and (D) TiO_2–$AC_{900\text{-}10}$.

The AC_{800} and AC_{900} samples present similar behaviour, whereas TiO_2 and particularly ZnO adsorb 2-propanol much less significantly than does the AC material (see Fig. 7(A)).

It is worth noting that AC_{900} sample was able to adsorb a higher amount of 2-propanol with respect to AC_{800}, although the latter presents a higher surface area. In several previous works [5–10,21,22] we have shown that the most important parameter which controls the adsorption of Brönsted acids corresponds to its zeta potential. In other words, surface pH of activated carbon instead of the surface area plays the most important role which controls the adsorption ability. In the present case, AC_{900} has a higher PZC and concomitantly a higher 2-propanol adsorption ability than that on AC_{800}.

Fig. 7(B) and (C) shows the adsorption ability of the composite powders based on TiO_2 and ZnO, respectively. In both cases the 5:1 powders, containing more AC, adsorb more 2-propanol than the 10:1 ones. The presence of AC_{800} or AC_{900} does not virtually modify the TiO_2 adsorption ability when the relative amount is 10:1 (see Fig. 7(B)), however the behaviour of the binary material is almost the same as that of the bare AC when the relative amount semiconductor:AC is 5:1. For the composites containing ZnO, Fig. 7(C), the behaviour is analogous to those materials containing TiO_2, i.e. the 10:1 samples absorption behaviour is slightly higher but very similar to the bare ZnO, whereas the 5:1 material behaves similarly to the correspondent bare AC although the amount of adsorbed 2-propanol was less significant.

The maximum number of 2-propanol adsorbed moles onto the surface of the catalysts were indicated as n_t and are reported in Table 2.

As it can be observed from the data reported in Table 2, the n_t figures of the binary materials are smaller than those obtained by summing the contribution of the bare TiO_2 or ZnO with that of AC. The results suggest the absence of additive effects in 2-propanol adsorption under dark conditions. This finding can be explained by considering that an interaction between the TiO_2 or ZnO particles and the AC ones occurs, establishing a contact interface. This contact area, indicated in the following as ΔS, could be not accessible to 2-propanol molecules and consequently the total number of adsorbed molecules for the substrate under dark conditions decreases. ΔS values for each binary material can be estimated by considering that the amount of 2-propanol that does not adsorb, due to the presence of the contact interface between the semiconductor and AC (amount indicated as Δn and named *dilution factor*), is related to ΔS and to the total surface density of the adsorbed 2-propanol onto the semiconductor ($d_{\text{surf-semiconductor}}$) and onto AC ($d_{\text{surf-AC}}$). Indeed, Δn for each binary material can be determined from the difference between the sum of the total number of adsorbed moles (n_t) on the bare semiconductor and on the bare AC, minus the n_t value obtained for the binary material:

$$\Delta n = [(n_{\text{t-semiconductor}} + n_{\text{t-AC}}) - (n_{\text{t-semiconductor-AC}})]. \quad (1)$$

Δn can be expressed also as:

$$\Delta n = \Delta S \times d_{\text{surf-semiconductor}} + \Delta S \times d_{\text{surf-AC}} \quad (2)$$

and consequently ΔS for each binary material can be calculated as:

$$\Delta S = \frac{\Delta n}{d_{\text{surf-semiconductor}} + d_{\text{surf-AC}}} \quad (3)$$

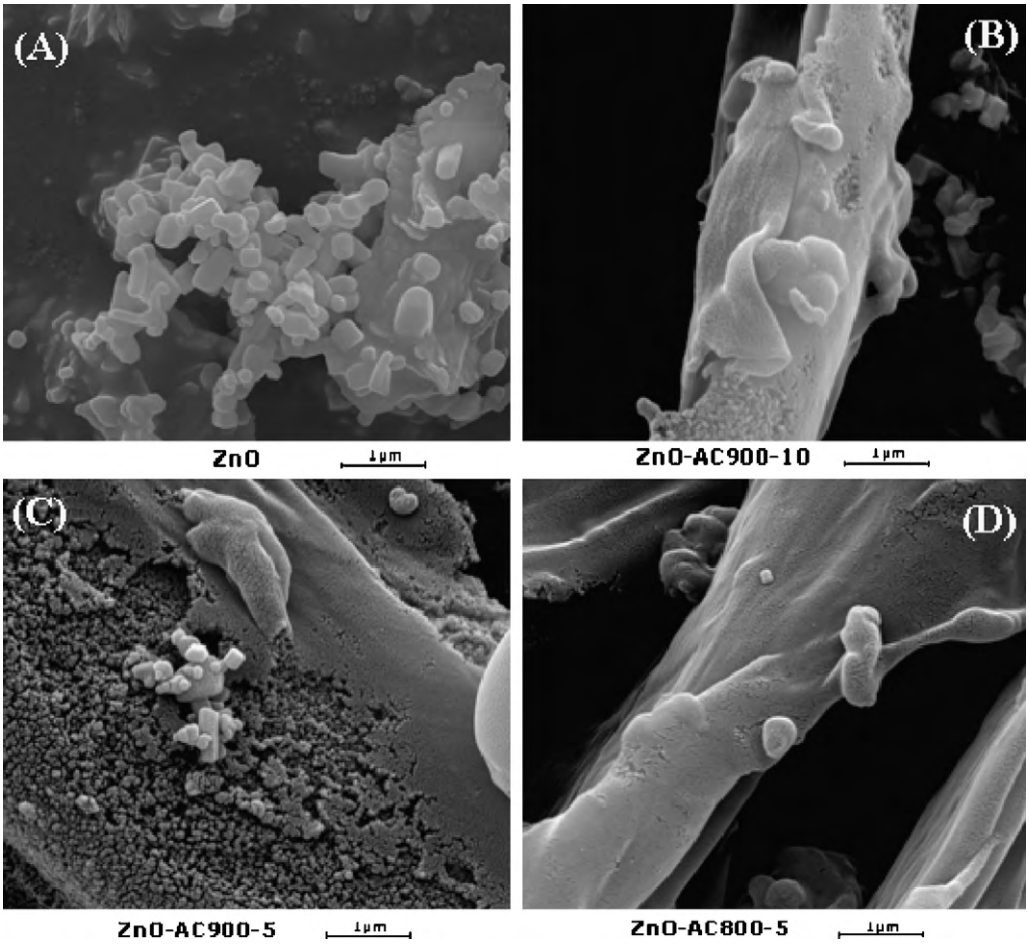

Fig. 4. SEM micrographs of (A) bare ZnO; (B) ZnO–$AC_{900\text{-}10}$; (C) ZnO–$AC_{900\text{-}5}$; and (D) ZnO–$AC_{800\text{-}5}$.

The total surface density of adsorbed 2-propanol values, d_{surf}, for bare AC both at 800 and 900 °C and for bare TiO_2 and bare ZnO were calculated as the ratio between the total number of adsorbed moles and the surface area corresponding to the amount of solid used during the dark adsorption experiments:

$$d_{surf\text{-}i} = \frac{n_{t\text{-}i}}{S_{BET\text{-}i} \times m_i} \quad (4)$$

where $n_{t\text{-}i}$ corresponds to the total number of adsorbed moles, $S_{BET\text{-}i}$ to the specific surface area and m_i to the weight of solid used during the dark adsorption experiment. The letter i indicates that the density can be calculated both for the semiconductors and for AC samples.

The three parameters concerning the synergy between the semiconductor and the AC, i.e. Δn, d_{surf} and ΔS are reported in Table 2.

From the study of the Δn values obtained for the binary material, it can be observed that the higher the mass of semiconductor (both TiO_2 and ZnO) used in the binary materials, the lower the Δn value.

It is worth mentioning that, although the total amount of 2-propanol adsorbed onto TiO_2 is clearly higher than that of ZnO (63 μmol against 10 μmol), the d_{surf} values corresponding to these two semiconductors are very similar (13.94 against 16.13 μmol m^{-2}). Moreover, d_{surf} values for AC samples resulted much lower than those calculated for the bare semiconductors, indicating a higher accumulation of 2-propanol onto the surface

Table 2
Maximum or total number of adsorbed 2-propanol moles (n_t) under dark conditions for the bare AC powders and the binary samples containing TiO_2 and ZnO, dilution factor (Δn), total surface density (d_{surf}) and contact interface (ΔS) between the solids.

Sample	$n_t \times 10^6$ (mol)	$\Delta n \times 10^6$ (mol)	$d_{surf} \times 10^6$ (mol m^{-2})	ΔS (m^2)
AC_{800}	90	–	4.77	–
AC_{900}	100	–	5.51	–
TiO_2	63	–	13.94	–
TiO_2–$AC_{800\text{-}10}$	75	33	–	1.76
TiO_2–$AC_{800\text{-}5}$	97	56	–	3.00
TiO_2–$AC_{900\text{-}10}$	80	33	–	1.70
TiO_2–$AC_{900\text{-}5}$	107	56	–	2.88
ZnO	10	–	16.13	–
ZnO–$AC_{800\text{-}10}$	20	35	–	1.67
ZnO–$AC_{800\text{-}5}$	51	49	–	2.34
ZnO–$AC_{900\text{-}10}$	33	27	–	1.25
ZnO–$AC_{900\text{-}5}$	67	43	–	2.00

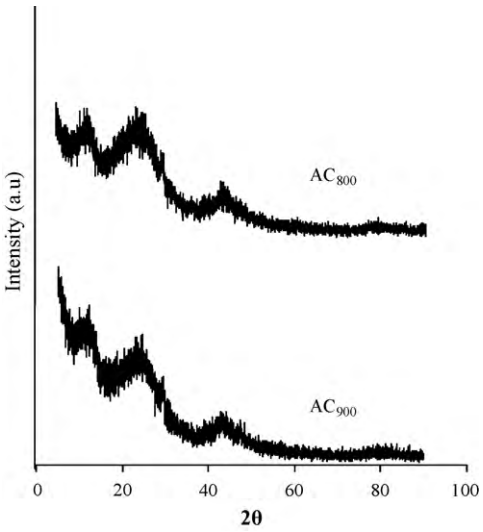

Fig. 5. XRD patterns of bare activated carbons.

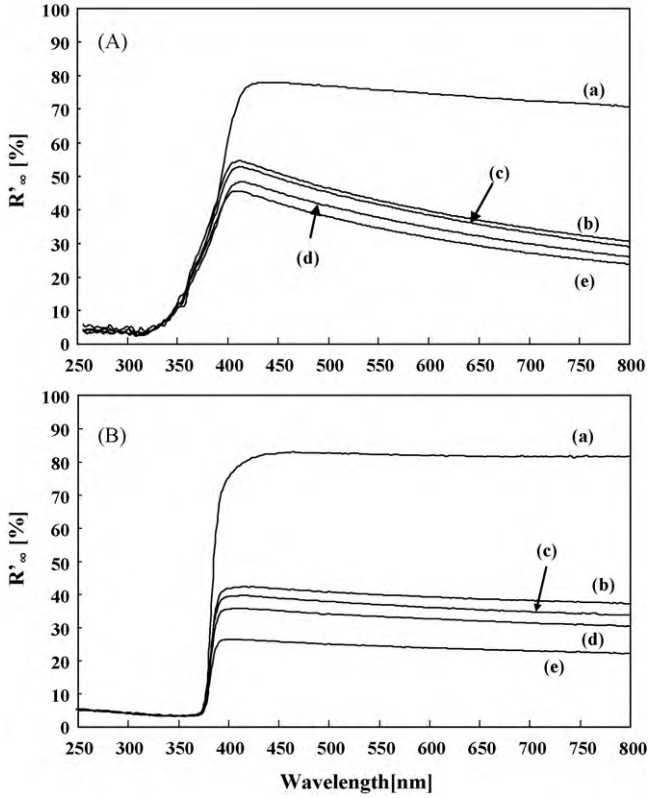

Fig. 6. Diffuse reflectance spectra of (A): (a) bare Degussa P25 TiO_2; (b) TiO_2–$AC_{900\text{-}10}$; (c) TiO_2–$AC_{800\text{-}10}$; (d) TiO_2–$AC_{900\text{-}5}$; (e) TiO_2–$AC_{800\text{-}5}$ and (B): (a) bare ZnO; (b) ZnO–$AC_{900\text{-}10}$; (c) ZnO–$AC_{800\text{-}10}$; (d) ZnO–$AC_{900\text{-}5}$; (e) ZnO–$AC_{800\text{-}5}$.

of these last solids and in particular onto ZnO. As evidenced from the data reported in Table 2, the higher the semiconductor mass in the binary material, the lower the common contact interface, ΔS, created between the solids. Therefore, the contact area, ΔS, increases by increasing the AC amount in the binary material. Moreover, ΔS is higher for the TiO_2–AC samples than for the ZnO–AC ones, according to the SEM micrographs where it can be observed that TiO_2 is better deposited onto the AC surface than ZnO does. The similar PZCs of AC_{800} and AC_{900} with that of ZnO (Table 1) could be responsible for a bad dispersion of ZnO particles onto AC and therefore for a smaller contact interface than that of TiO_2–AC materials.

3.3. Photocatalytic degradation of 2-propanol in gas–solid regime

Preliminary runs were performed under the same experimental conditions used for the photoreactivity experiments but in the absence of catalyst, oxygen or light. No reactivity was observed in all these cases, so it was concluded that the simultaneous presence of O_2, catalyst, and irradiation is needed for the occurrence of 2-propanol degradation process. Moreover, it is worth noting that the bare AC powders evidenced no photocatalytic activity under the experimental conditions employed. The photoreactivity runs started when the system achieved the steady state condition under dark. Fig. 8(A) and (B) reports the values of the 2-propanol concentration versus irradiation time for runs carried out by using bare TiO_2 and bare ZnO, respectively.

Figs. 9 and 10 report the photocatalytic activity of the binary materials based on TiO_2 and ZnO, respectively.

2-Propanol in gas phase completely disappeared after the photocatalytic reaction by using all the solids containing TiO_2. Throughout all the runs the decrease in the substrate concentration was observed along with a simultaneous formation of propanone and acetaldehyde, which were found as the major and the minor organic intermediate products, respectively. Moreover carbon dioxide was also produced.

In particular, it is worth noting that the amount of 2-propanol decreased until zero in the first hour of irradiation in the presence of bare TiO_2, and concomitantly propanone and acetaldehyde con-

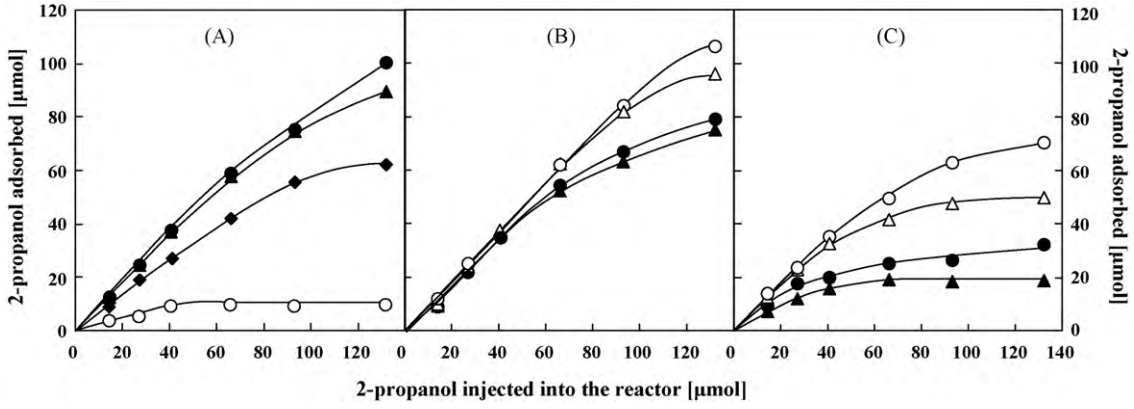

Fig. 7. Amount of 2-propanol adsorbed versus that injected in the reactor in the presence of (A): (♦) TiO_2 Degussa P25; (▲) AC_{800}; (●) AC_{900}; (○) ZnO; (B): (△) TiO_2–$AC_{800\text{-}5}$; (▲) TiO_2–$AC_{800\text{-}10}$; (○) TiO_2–$AC_{900\text{-}5}$; (●) TiO_2–$AC_{900\text{-}10}$; and (C): (△) ZnO–$AC_{800\text{-}5}$; (▲) ZnO–$AC_{800\text{-}10}$; (○) ZnO–$AC_{900\text{-}5}$; (●) ZnO–$AC_{900\text{-}10}$.

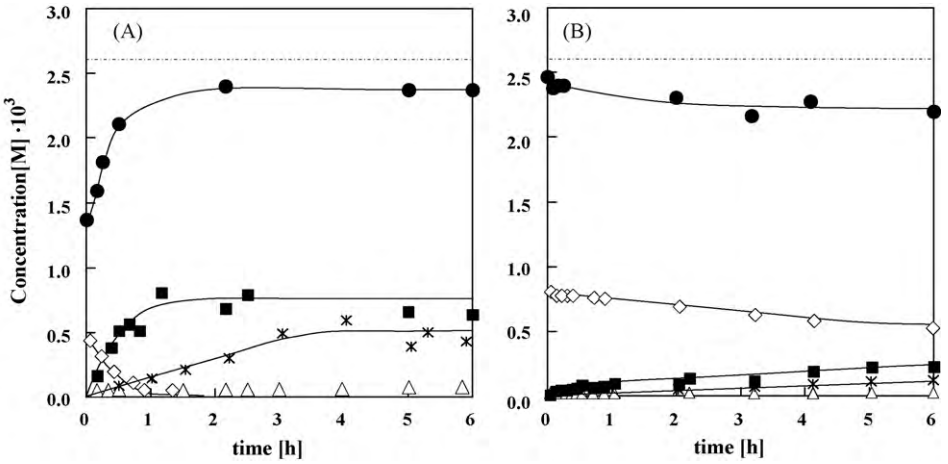

Fig. 8. Evolution of (◊) 2-propanol; (■) propanone; (△) acetaldehyde and (*) CO_2 along with the total concentration of carbon in the fluid phase (●) versus irradiation time for reaction in the gas–solid system in the presence of (A) TiO_2 Degussa P25 and (B) ZnO. The horizontal dotted line represents the total amount of carbon injected in the system.

centrations increased remaining almost constant throughout the run. Similarly, the amount of formed CO_2 increased only during the first three hours of irradiation, remaining constant during the further three hours (see Fig. 8(A)). This finding can be attributed to deactivation of the TiO_2 surface by adsorption of organic and/or carbonate species. The deactivation of TiO_2 P25 in reactions carried out in gas phase was already reported in others works [29,30]. As far as ZnO is concerned, its photocatalytic activity is much lower than that of TiO_2. Indeed only a slow degradation of 2-propanol occurred (see Fig. 8(B)) and only very small amounts of intermediates and CO_2 formed. Anyway no deactivation of ZnO was observed.

Fig. 8(A) and (B) also shows the total amount of carbon in the system (in the gas phase), indicating that it is always smaller compared to the stoichiometric one; this behaviour suggests that some

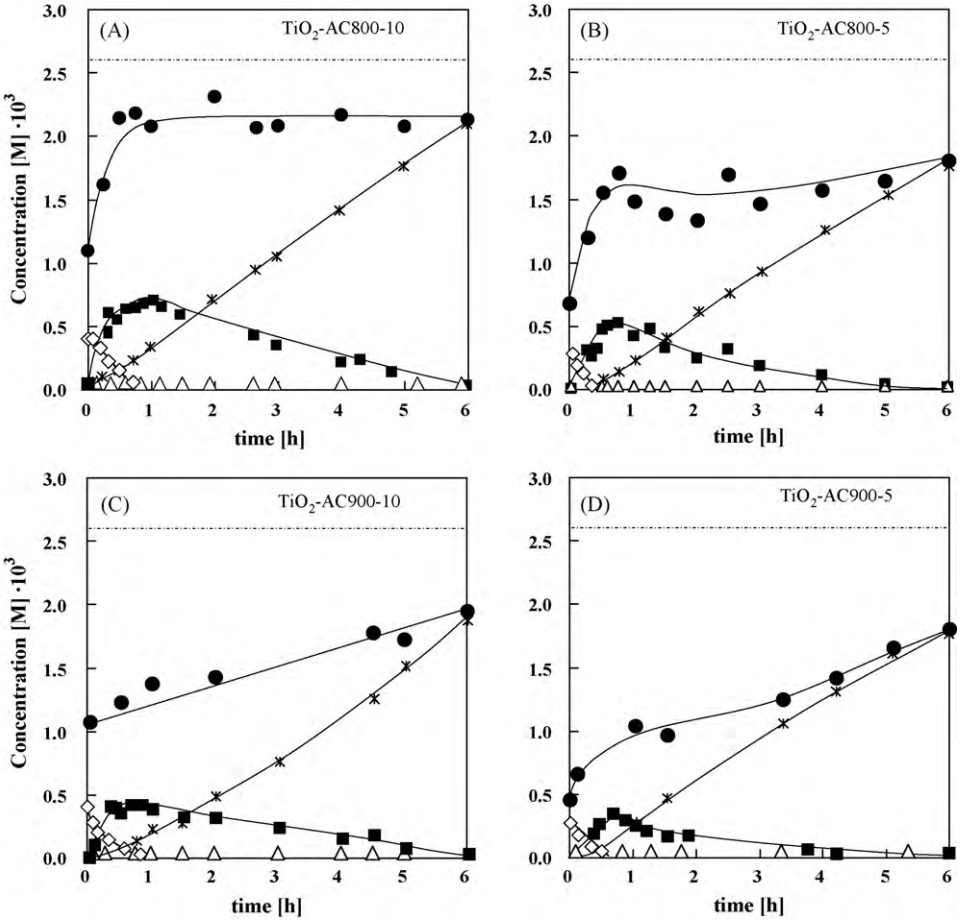

Fig. 9. Evolution of (◊) 2-propanol; (■) propanone; (△) acetaldehyde and (*) CO_2 along with the total concentration of carbon in the fluid phase (●) versus irradiation time for reaction in the gas–solid system in the presence of (A) TiO_2–$AC_{800\text{-}10}$; (B) TiO_2–$AC_{800\text{-}5}$; (C) TiO_2–$AC_{900\text{-}10}$ and (D) TiO_2–$AC_{900\text{-}5}$. The horizontal dotted line represents the total amount of carbon injected in the system.

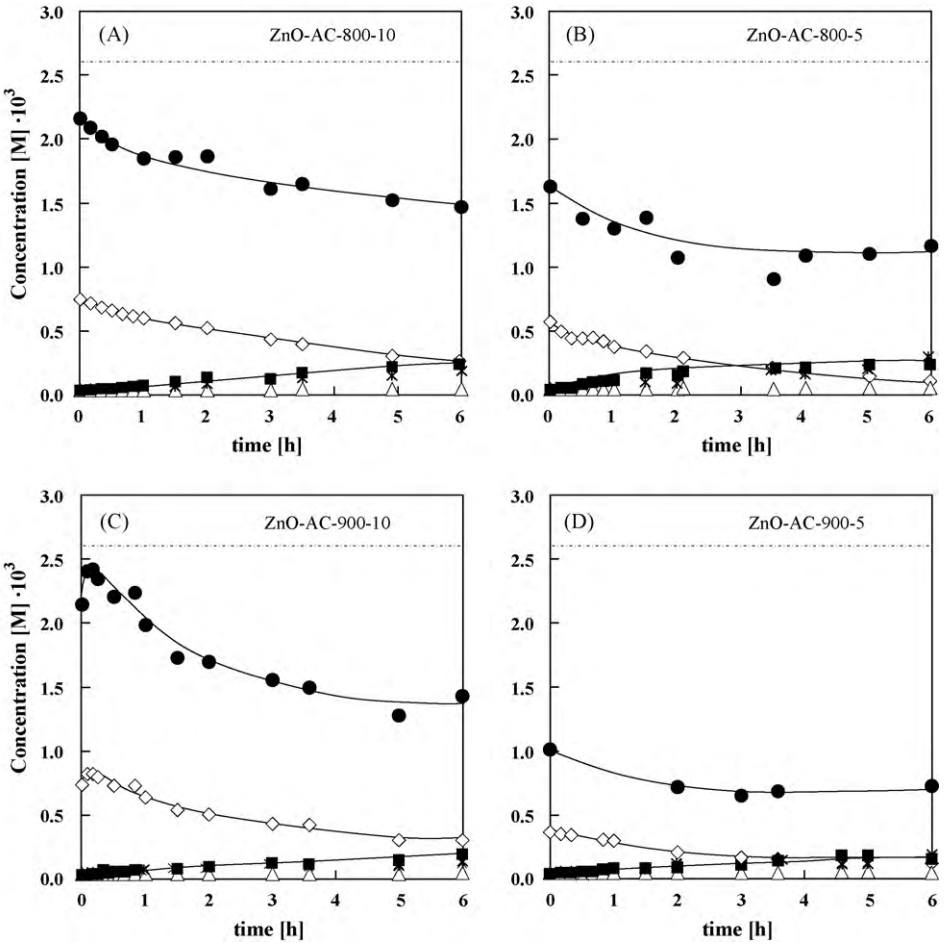

Fig. 10. Evolution of (◊) 2-propanol; (■) propanone; (△) acetaldehyde and (*) CO_2 along with the total concentration of carbon in the fluid phase (●) versus irradiation time for reaction in the gas–solid system in the presence of (A) ZnO–$AC_{800\text{-}10}$; (B) ZnO–$AC_{800\text{-}5}$; (C) ZnO–$AC_{900\text{-}10}$ and (D) ZnO–$AC_{900\text{-}5}$. The horizontal dotted line represents the total amount of carbon injected in the system.

species (organic and/or inorganic) remain adsorbed on the solid surface.

In the presence of both TiO_2–AC and ZnO–AC binary materials (Figs. 9 and 10) the concentration of 2-propanol decreased, whereas the concentrations of propanone and acetaldehyde increased during the irradiation. Nevertheless, in the presence of TiO_2–AC samples propanone concentration initially increased and after a time ranging between 0.5 and 1 h started to decrease. The photocatalytic activity in the presence of TiO_2–AC is much higher than that showed in the presence of bare TiO_2. In fact 2-propanol disappeared very quickly after the starting of irradiation. In respect to the conversion to CO_2, the presence of AC influences also the performance of the semiconductor; indeed, binary materials were able, in some cases, to almost completely degrade 2-propanol, while the bare TiO_2, due to its deactivation, was able to degrade it only partially. The reactivity of ZnO–AC was much lower than that of TiO_2–AC materials and analogously to what was observed with pure ZnO, 2-propanol slowly disappeared while propanone, acetaldehyde and CO_2 appeared only in very low amounts during the course of the runs. The presence of AC in the ZnO–AC materials gave rise, also in this case, to an increase in the photocatalytic performance of the bare ZnO.

From the observation of Figs. 9 and 10 as in the case of Fig. 8, it is evident that the total amount of carbon in the system was always smaller compared to the stoichiometric one, indicating that some species (organic and/or inorganic) remain adsorbed on the solid surface at least after the duration (6 h) of the experiments. The loss of total carbon present in gas phase, for runs carried out in the presence of binary materials, was higher compared to that observed in the presence of the bare semiconductor.

This finding is clearly due to the presence of AC that can adsorb more amounts of species (organic and/or inorganic) with respect to TiO_2 and ZnO. When the binary materials were used, the CO_2 concentration always increased throughout the runs, indicating that no deactivation of the catalyst occurred.

To verify if catalyst deactivation occurs, the most active material, i.e. TiO_2–$AC_{800\text{-}10}$, was tested for three consecutive experiments that lasted a longer time (ca. 11 h) with respect to the other ones (see Fig. 11). No significant deactivation of the photocatalyst was observed.

Notably CO_2 evolution after 7–8 h of irradiation reached a value corresponding to ca. 98% of the carbon present in the injected 2-propanol, indicating that no oxidation of AC to CO_2 occurred during the photocatalytic runs.

Due to the high adsorption of 2-propanol on the catalyst surface it was not possible to confidentially study the kinetics of photodegradation of 2-propanol; consequently the photoactivity of the various samples was compared by calculating the rate of CO_2 evolution. For all of the catalysts the evolution of CO_2 in the fluid phase started with illumination, indicating that mineralization of the substrate occurred in the first steps of the photoreaction. Zero order kinetics was found for all the runs at least during the first two hours of irradiation. CO_2 evolution rates (r_0) calculated for each catalyst are showed in Table 3 along with an important

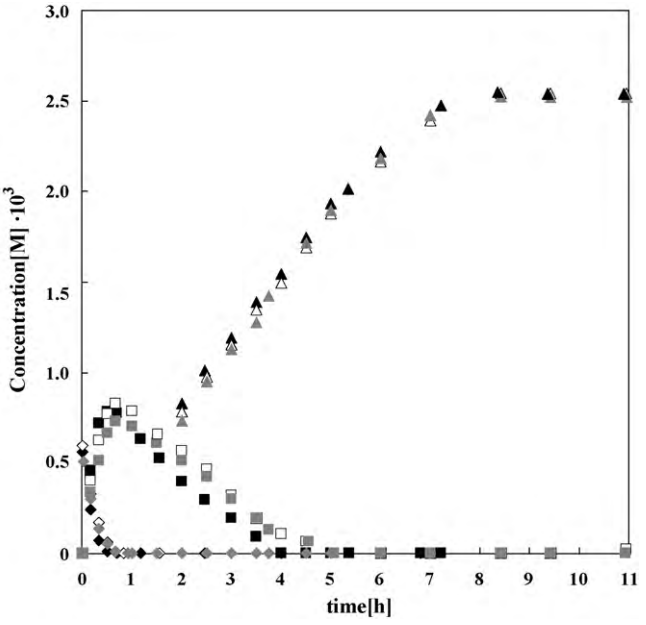

Fig. 11. Evolution of (♦, ◊, ◆) 2-propanol; (■, □, ■) propanone and (▲, △, ▲) CO_2 versus irradiation time for reaction in the gas–solid system in the presence of TiO_2–$AC_{800\text{-}10}$ for three consecutive runs. First run: black symbols, second run: empty symbols and third run: grey symbols.

parameter, I_F, recently reported by some of us as an interaction factor [6,10,21] and the percentage of conversion to CO_2 after 6 h irradiation.

CO_2 percentage conversion was obtained by dividing the concentration of CO_2 in gas phase measured after 6 h of irradiation by the stoichiometric value deriving from the complete oxidation of the initial 2-propanol.

I_F values enable to establish whether a synergy or an inhibition effect occurs between the components of the binary materials. They were determined by means of the following equation:

$$I_F = \frac{r_{0\,\text{semiconductor-AC}}}{r_{0\,\text{semiconductor}} + r_{0\,\text{AC}}} \quad (5)$$

where $r_{0\,\text{semiconductor-AC}}$ and $r_{0\,\text{semiconductor}}$ are the CO_2 evolution rates obtained in the experiments carried out in the presence of the mixed solids and in the presence of the bare semiconductor (TiO_2 or ZnO), respectively, and $r_{0\,\text{AC}}$ should be the CO_2 evolution rates related to a possible activity of the bare AC powder. Nevertheless the last term can be neglected because AC is not photocatalytically active. The perusal of Table 3 indicates that the r_0 values were always higher for all the binary materials with respect to the bare semiconductors, showing a beneficial effect of the presence of AC that was confirmed by synergy factors, $I_F > 1$.

Table 3
Evolution rate of CO_2 (r_0), interaction factor between solids (I_F) and conversion percentage to CO_2 after 6 h of irradiation.

Photocatalyst	$r_0 \times 10^7$ (M min^{-1})	I_F	Conversion to CO_2 (%)
AC_{800}	n.a.[a]	–	n.a.[a]
AC_{900}	n.a.[a]	–	n.a.[a]
TiO_2	24[b]	1	23.2
TiO_2–$AC_{800\text{-}10}$	60	2.5	77.0
TiO_2–$AC_{800\text{-}5}$	52	2.2	68.0
TiO_2–$AC_{900\text{-}10}$	54	2.3	73.0
TiO_2–$AC_{900\text{-}5}$	52	2.2	68.0
ZnO	2.2	1	2.9
ZnO–$AC_{800\text{-}10}$	4.2	1.9	5.9
ZnO–$AC_{800\text{-}5}$	5.0	2.3	7.1
ZnO–$AC_{900\text{-}10}$	2.6	1.2	3.6
ZnO–$AC_{900\text{-}5}$	2.9	1.3	3.9

[a] Not active.
[b] Due to the TiO_2 deactivation, the figure is calculated during the two first hours of irradiation.

No significative differences on the photoactivity were observed when the ratio semiconductor:AC was 5:1 or 10:1 at both the activation temperatures (800 and 900 °C), although the TiO_2–$AC_{800\text{-}10}$ sample resulted the most active one.

Finally, the results reported in Table 3 reveal that the presence of AC in TiO_2–AC binary materials enormously increased the photocatalytic ability of the bare semiconductor in the substrate complete oxidation to CO_2. Bare TiO_2 deactivated during the first three hours of irradiation, probably due to the strong adsorption onto its surface of organics and/or carbonate species. On the contrary, when AC was present, the majority of the substrate and the intermediates species was reversibly adsorbed onto the AC surface [8], maintaining clear and consequently very active TiO_2 surface. Due to the presence of a contact interface between TiO_2 and AC, a continuous transfer of the species from AC to TiO_2 surface probably by means of various adsorption–desorption steps involving both surfaces was possible. This picture is also supported by the fact that the amount of CO_2 produced always increased with the reaction time (see Fig. 9), indicating that no deactivation of TiO_2 occurred in the binary materials. The fact that the surface was always active gave rise to the complete oxidation of the substrates avoiding the accumulation of carboxylate species on TiO_2 surface.

Similarly, in the case of ZnO–AC materials also, an increase in the complete oxidation of 2-propanol to CO_2 was observed, but, due to the intrinsic low photoactivity of the zinc oxide sample used, the photoactivity of the ZnO–AC samples showed to be very low always.

To investigate the influence of the presence of H_2O vapour both on the photodegradation and deactivation processes, two experiments were carried out. The first with the bare Degussa P25 TiO_2 photocatalyst that underwent deactivation in the absence of water and the second with the most active binary material, i.e. TiO_2–$AC_{800\text{-}10}$. For both cases, in the presence of H_2O vapour at concentration similar to the initial concentration of 2-propanol, we did not observe differences in photoreactivity with respect to runs carried out in the absence of H_2O vapour. It can be concluded that the presence of water vapour does not influence the performance of the solid photocatalysts in accordance with previous literature [12], at least under the experimental conditions used. This finding can be explained by considering the fact that the quantity of water produced during the reaction is sufficient to allow the restoration of the active sites [13–15].

4. Conclusions

The photocatalytic degradation of 2-propanol occurred successfully in gas–solid regime by using both commercial TiO_2 and ZnO and home-prepared TiO_2–AC and ZnO–AC binary materials. In general, TiO_2–AC binary samples were more photoactive than the ZnO–AC ones. In all cases propanone was the major intermediate, acetaldehyde the minor one and carbon dioxide the final oxidation product. Photoreactivity experiments showed that the presence of AC along with TiO_2 in the binary materials enormously increased the photocatalytic ability of the bare semiconductor to oxidize the substrate to CO_2, clearly indicating a synergy between the semiconductor and AC. In particular the evolution rate of CO_2 deriving from the complete oxidation of 2-propanol was 2.2–2.5 times faster by using TiO_2–AC than that using the bare TiO_2 sample. Moreover the presence of AC avoided the deactivation of TiO_2 that occurred when the bare semiconductor was used. The evolution rate of CO_2 in the presence of ZnO–AC samples, instead, increased up to ca. 2.3 times with respect to that observed for the bare ZnO, although the photoactivity showed to be always very low.

Acknowledgements

The authors wish to thank MIUR (Rome) and Università degli Studi di Palermo for financial support.

References

[1] M. Schiavello (Ed.), Photocatalysis and Environment. Trends and Applications, Kluwer, Dordrecht, 1988.
[2] A. Fujishima, K. Hashimoto, T. Watanabe, TiO_2 Photocatalysis. Fundamentals and Applications, BKC Inc., Tokyo, 1999.
[3] A. Fujishima, T.N. Rao, D.A. Tryk, J. Photochem. Photobiol., C 1 (2000) 1–21.
[4] F. Rodriguez-Reinoso, Carbon 36 (1998) 159–175.
[5] J. Matos, J. Laine, J.-M. Herrmann, D. Uzcategui, J.L. Brito, Appl. Catal., B 70 (2007) 461–469.
[6] T. Cordero, C. Duchamp, J.M. Chovelon, C. Ferronato, J. Matos, J. Photochem. Photobiol., A 191 (2007) 122–131.
[7] J.-M. Herrmann, J. Matos, J. Disdier, C. Guillard, J. Laine, S. Malato, J. Blanco, Catal. Today 54 (1999) 255–265.
[8] J. Matos, J. Laine, J.-M. Herrmann, J. Catal. 200 (2001) 10–20.
[9] J. Matos, J. Laine, J.-M. Herrmann, Appl. Catal., B 18 (1998) 281–291.
[10] J. Matos, A. García, T. Cordero, J.M. Chovelon, C. Ferronato, Catal. Lett. 130 (2009) 568–574.
[11] E. Pulido Malián, O. González Díaz, J.M. Doña Rodríguez, G. Colón, J. Araña, J. Herrera Melián, J.A. Navío, J. Pérez Peña, Appl. Catal., A 364 (2009) 174–181, and references therein.
[12] G. Marcì, E. García-López, G. Mele, L. Palmisano, G. Dyrda, R. Słota, Catal. Today 143 (2009) 203–210.
[13] R.I. Bickley, G. Munuera, F.S. Stone, J. Catal. 31 (1973) 398–407.
[14] S.A. Larson, J.A. Widengree, J. Falconer, J. Catal. 157 (1995) 611–625.
[15] F. Arsac, D. Bianchi, J.M. Chovelon, C. Ferronato, J.-M. Herrmann, J. Phys. Chem. A 110 (2006), 4202–4212 and 4213–4222.
[16] B. Othani, K. Iwai, S. Nishimoto, S. Sato, J. Phys. Chem. B 101 (1997) 3349–3359.
[17] A. Sclafani, J.-M. Herrmann, J. Photochem. Photobiol., A 113 (1998) 181–188.
[18] H. Yamashita, Y. Nishida, S. Yuan, K. Mori, M. Nirisawa, Y. Matsumura, T. Ohmichi, I. Takayama, Catal. Today 120 (2007) 163–167.
[19] E. Ortiz-Islas, T. López, J. Navarrete, X. Bokhimi, R. Gómez, J. Mol. Catal. A: Chem. 228 (2005) 345–350.
[20] G. Marcì, E. García-López, L. Palmisano, D. Carriazo, C. Martin, V. Rives, Appl. Catal., B 90 (2009) 497–506.
[21] T. Cordero, J.M. Chovelon, C. Duchamp, C. Ferronato, J. Matos, Appl. Catal., B 73 (2007) 227–235.
[22] J. Matos, M. Labady, A. Albornoz, J. Laine, J.L. Brito, J. Mol. Catal. A: Chem. 228 (2005) 189–194.
[23] M.V. Lopez-Ramon, F. Stoeckli, C. Moreno-Castilla, F. Carrasco-Marin, Carbon 37 (1999) 1215–1221.
[24] A. Sedlak, W. Janusz, Physicochem. Probl. Miner. Process. 42 (2008) 57–66.
[25] (a) R.I. Bickley, T. González-Carreño, J.S. Lees, L. Palmisano, R.J.D. Tilley, J. Solid State Chem. 92 (1991) 178–190;
(b) Y. Wang, G. Zhou, T. Li, W. Qiao, Y. Li, Catal. Commun. 10 (2009) 412–415.
[26] F.P. Koffyberg, K. Dwight, A. Wald, Solid State Commun. 30 (1979) 433–437.
[27] C. Wang, Q. Li, B. Mao, E. Wang, C. Tian, Mater. Lett. 62 (2008) 1339–1341.
[28] J. Torrent, V. Barrón, Encyclopedia of Surface and Colloidal Science, Marcel Dekker Inc., New York, 2002.
[29] G. Marcì, M. Addamo, V. Augugliaro, S. Coluccia, E. García-López, V. Loddo, G. Martra, L. Palmisano, M. Schiavello, J. Photochem. Photobiol., A 160 (2003) 105–114.
[30] J. Araña, J.M. Doña Rodríguez, C. Garriga i Cabo, O. González Díaz, J.A. Herrera Melián, J. Pérez Peña, Appl. Catal., B 53 (2004) 221–232.